AJNR

Evaluation of Brain and Head and Neck Tumors with 4D Contrast-Enhanced MR Angiography at 3T

S. Nishimura, T. Hirai, Y. Shigematsu, M. Kitajima, M. Morioka, Y. Kai, R. Minoda, H. Uetani, R. Murakami and Y. Yamashita

AJNR Am J Neuroradiol 2012, 33 (3) 445-448
doi: https://doi.org/10.3174/ajnr.A2819
http://www.ajnr.org/content/33/3/445

ORIGINAL RESEARCH

S. Nishimura
T. Hirai
Y. Shigematsu
M. Kitajima
M. Morioka
Y. Kai
R. Minoda
H. Uetani
R. Murakami
Y. Yamashita

Evaluation of Brain and Head and Neck Tumors with 4D Contrast-Enhanced MR Angiography at 3T

BACKGROUND AND PURPOSE: Systematic assessment of brain and head and neck tumors with 4D-CE-MRA at 3T has not been investigated. The purpose of this study was to test the hypothesis that 4D-CE-MRA at 3T can replace DSA in the identification of feeding arteries and tumor stain to plan interventional procedures in hypervascular brain and head and neck tumors.

MATERIALS AND METHODS: Fifteen consecutive patients with brain and head and neck tumors underwent 4D-CE-MRA at 3T and DSA. 4D-CE-MRA combined randomly segmented central *k*-space ordering, keyhole imaging, SENSE, and half-Fourier imaging. We obtained 30 dynamic scans every 1.9 seconds at an acquired spatial resolution of 0.9 × 0.9 × 1.5 mm; the matrix was 256 × 256. Two independent observers inspected the 4D-CE-MRA images for the main arterial feeders and tumor stain. Interobserver and intermodality agreement was assessed by κ statistics.

RESULTS: For 4D-CE-MRA, the interobserver agreement was fair with respect to the main arterial feeders and very good for the degree of tumor stain (κ = 0.28 and 0.87, respectively). Intermodality agreement was moderate for the main arterial feeders (κ = 0.45) and good for the tumor stain (κ = 0.74).

CONCLUSIONS: Although 4D-CE-MRA may be useful for evaluating tumor stain in hypervascular brain and head and neck tumors, it is not able to replace DSA in planning interventional procedures.

ABBREVIATIONS: CE-MRA = contrast-enhanced MRA; CENTRA = contrast-enhanced robust-timing angiography; CI = confidence interval; SENSE = sensitivity encoding

In patients with hypervascular brain and head and neck tumors (eg, meningiomas, juvenile nasopharyngeal angiofibromas, and paragangliomas), tumor embolization is considered a useful preoperative adjuvant therapy to mitigate blood loss during subsequent surgical resection.[1] To determine the need for preoperative embolization, one must understand the tumor vasculature.

Intra-arterial DSA remains the criterion standard for assessing the vasculature of hypervascular tumors of the brain and head and neck regions. Its inherent high spatial and temporal resolution facilitates the identification of the feeding arteries and the vascularity of the tumors. However, because DSA is invasive, exposes the patient to radiation, and requires the injection of iodinated contrast material, a noninvasive method is preferable for the accurate diagnosis of these tumors, including preinterventional and presurgical evaluations.

Although conventional MR imaging, time-of-flight MRA, and contrast-enhanced MRA have been used in the noninvasive evaluation of tumor vascularity,[2-4] their failure to yield hemodynamic information limits their clinical usefulness. Head and neck tumors have been diagnosed by time-resolved contrast-enhanced MRA at 1.5T.[5-7] This technique combines the T1 shortening effect of gadolinium-based contrast agents, dynamic imaging, and digital subtraction and parallel imaging techniques and yields MRA images of high temporal resolution.[5-7] Although the use of 3T for assessing various lesions in the brain and head and neck regions by 4D-CE-MRA has been described,[8-10] to our knowledge, systematic evaluation of this method in patients with brain and head and neck tumors has not been performed. MR imaging scanners at 3T provide a high signal intensity–to-noise ratio. Temporal and spatial resolution can be further improved by applying the intelligent *k*-space sampling techniques (ie, CENTRA, parallel imaging, and partial Fourier imaging).[8-14] The purpose of this study was to test the hypothesis that 4D-CE-MRA with the CENTRA keyhole method, parallel imaging, and half-scan at 3T can replace DSA in the identification of feeding arteries and tumor stain to plan interventional procedures in hypervascular brain and head and neck tumors.

Received April 25, 2011; accepted after revision June 29.

From the Departments of Diagnostic Radiology (S.N., T.H., Y.S., M.K., H.U., Y.Y.), Neurosurgery (M.M., Y.K.), and Otolaryngology-Head and Neck Surgery (R. Minoda), Graduate School of Medical Sciences, Kumamoto University, Kumamoto, Japan; and Department of Medical Imaging (R. Murakami), Faculty of Life Sciences, Kumamoto University, Kumamoto, Japan

Please address correspondence to Toshinori Hirai, Department of Diagnostic Radiology, Graduate School of Medical Sciences, Kumamoto University, 1–1-one Honjo, Kumamoto 860-8556 Japan; e-mail: t-hirai@kumamoto-u.ac.jp

http://dx.doi.org/10.3174/ajnr.A2819

Materials and Methods

Study Population

Our study was approved by our institutional review board, and informed consent for imaging examinations was obtained from all patients or their relatives. The study included 15 consecutive patients, 10 men and 5 women, ranging in age from 26 to 77 years (mean, 58.3 years), with brain and head and neck tumors who underwent 4D-CE-MRA and DSA between February 2008 and February 2010.

Of the 15 tumors, 4 were meningiomas; 3 were hemangioblastomas; 2 each were buccal cancers and hemangiomas; and 1 each was a juvenile angiofibroma, a metastatic bone tumor from hepatocellular carcinoma, a nasal cavity carcinoma, and a central neurocytoma. Fourteen were newly diagnosed, and 1 was a residual postembolization meningioma. In 14 patients, the interval between DSA and 4D-CE-MRA ranged from 1 to 14 days (mean, 7 days); in the patient with

juvenile angiofibroma, the interval was 83 days. The maximum tumor diameter ranged from 33 to 94 mm (mean, 51 mm).

DSA Technique

After catheterization of the internal and external carotid and vertebral arteries via the femoral artery approach, a trained neuroradiologist or a neurosurgeon performed diagnostic biplanar intra-arterial DSA (Allura Xper FD; Philips Healthcare, Best, the Netherlands). The acquisition parameters were matrix, 1024 × 1024; FOV, 17 cm; 3 frames/s. For each projection, a 6- to 10-mL bolus of undiluted iodinated contrast material with an iodine concentration of 300 mg/mL (iopamidol, Iopamiron 300; Bayer-Schering, Berlin, Germany) was manually injected.

MR Imaging

4D-CE-MRA was performed on a 3T MR imaging system (Achieva; Philips Healthcare) by using a commercially available 8-channel head coil. The MR imaging unit was equipped with a gradient system that allowed a maximal achievable gradient amplitude of 40 mT/m, a rise time of 0.2 ms, and a slew rate of 200 T/m/s.

The patients were positioned with a 20-ga intravenous catheter inserted into the antecubital vein. The intravenous injection of 0.2 mL of gadopentetate dimeglumine (Magnevist; Bayer-Schering) per kilogram of body weight (flow rate, 3 mL/s) was followed by a 30-mL saline flush delivered with an automated power injector. 4D-CE-MRA was started after injection of the contrast agent. The acquisition parameters for 4D-CE-MRA were the following: TR/TE, 2.9/1.4 ms; flip angle, 20°; image matrix, 256 × 256; FOV, 256 mm covering the entire head and face.

4D-CE-MRA was acquired by using a combination of the CENTRA keyhole method and the SENSE technique; a half-scan was used to improve temporal resolution at 4D-CE-MRA at a constant spatial resolution.[8-14] We acquired 120 thin sagittal partitions of 2 mm with a 1-mm overlap between sections by using a SENSE factor of 2 in the section-selection direction and of 4 in the phase-encoding direction and a keyhole diameter of 15%; this yielded a voxel size of 1.0 × 1.0 × 1.5 mm (1.5 mm^3) with zero-filling. In total, 24 dynamic volumes were acquired with an average keyhole imaging duration of 1.9 s/volume, followed by dynamic reference imaging with a duration of 3.9 seconds. The total acquisition time for the 4D-CE-MRA sequence was 50 seconds. Time-resolved MRA yielded a total acceleration factor of 88.8 (6.66 [15% keyhole] × 8 [SENSE] / 0.6 [half-scan factor]) compared with standard CE-MRA without such techniques.

Image processing included mask subtraction to suppress the background signal intensity of stationary tissue. Images were displayed with a reconstructed isotropic image matrix of 1 × 1 × 1 mm. Routine MR imaging included pre- and postcontrast T1-weighted spin-echo and T2-weighted fast spin-echo sequences.

Image Analysis

Two independent readers (T.H. and Y.K. with 21 and 24 years of experience in neuroangiography, respectively) qualitatively evaluated the whole series of DSA images on a PACS workstation. Divergent evaluations were reviewed to reach consensus. Two other readers (Y.S. and M.K., with 17 and 19 years of experience in neuroradiologic MR imaging, respectively) independently evaluated the 4D-CE-MRA data on a PACS workstation; they were blinded to clinical and DSA data. Divergent assessments were re-evaluated by the 2 readers to reach a consensus. On the PACS workstation, maximal-intensity-projection 4D-CE-MRA images were displayed on the anteroposterior, lateral, and axial views. The software allowed enlargement of regions of special interest in any given spatial orientation.

At first, the overall image quality of the 4D-CE-MRA studies was recorded by using a 3-point scale: class 3, class 2, and class 1. Class 3 meant that images had sufficient quality for interpretation and no or slight artifacts. Class 2 indicated that images had mild-to-moderate artifacts not interfering with interpretation. Class 1 meant that image quality was inadequate, and there were severe artifacts interfering with interpretation.

Visualization of the main arterial feeder and the degree of tumor stain were assessed on 4D-CE-MRA and conventional DSA images. Main arterial feeders were defined as branches from the internal maxillary, middle meningeal, facial, occipital, and ophthalmic arteries; the internal carotid, anterior, middle, and posterior cerebral arteries; the superior, anterior, inferior, and posterior inferior cerebellar arteries; and other arteries. The degree of tumor stain was classified as grade 0, not visible; grade 1, visible only after the late arterial phase; and grade 2, visible from the early arterial phase.

Statistical Analysis

Interobserver agreement between 2 readers of 4D-CE-MRA and DSA images and intermodality agreement between consensus readings of 4D-CE-MRA and DSA images with respect to the main arterial feeders and tumor stain were determined by calculating the κ coefficient ($\kappa < 0.20$ = poor; $\kappa = 0.21–0.40$, fair; $\kappa = 0.41–0.60$, moderate; $\kappa = 0.61–0.80$, good; $\kappa = 0.81–0.90$, very good; and $\kappa > 0.90$, excellent agreement). In addition, we recorded the exact number and percentage of times when results from the 2 readers and the 2 modalities were in exact agreement. A statistical package, MedCalc for Windows (MedCalc Software, Mariakerke, Belgium), was used for all analyses.

Results

In the qualitative evaluation of DSA, interobserver agreement was excellent for all items ($\kappa = 1.0$). Table 1 is a summary of the DSA and 4D-CE-MRA findings on the 15 tumors. On DSA images, 4 tumors were primarily supplied by the internal maxillary artery; 3, by the ophthalmic artery; 2, by the facial artery; 2, by the anterior cerebral artery; and 1 each, by the posterior cerebral artery, the posterior inferior cerebellar artery, the internal carotid artery, and by another feeder (ie, the posterior meningeal artery). Tumor stain on DSA images was grade 2 in 9 patients (60%) and grade 1 in the other 6.

The overall quality of all 4D-CE-MRA images was judged to be class 3. In 8 of 15 studies (53%), the consensual interpretation of 4D-CE-MRA and DSA images coincided with respect to the main arterial feeders (Table 1 and Fig 1). In 6 cases, the main arterial feeders depicted by DSA were not identified on 4D-CE-MRA images (Fig 2). Intermodality agreement (consensus reading of 4D-CE-MRA versus DSA images) was moderate ($\kappa = 0.45$; 95% CI, 0.17–0.74) (Table 2). In the analysis of the main arterial feeders, the 2 readers reviewing 4D-CE-MRA images agreed in 6 of 15 studies (40%); interobserver agreement was recorded as fair ($\kappa = 0.28$; 95% CI, 0.10–0.66) (Tables 1 and 2).

4D-CE-MRA and DSA tumor-stain findings were in agreement in 13 of the 15 patients (87%) (Figs 1 and 2). Intermodality agreement between DSA and 4D-CE-MRA was good ($\kappa = 0.74$; 95% CI, 0.41–1.0). Independently, the readers agreed on the degree of tumor stain in 14 cases (93%); agree-

Table 1: Summary of DSA and 4D-CE-MRA findings

	4D-CE-MRA					
	Observer 1	Observer 2	Interobserver Agreement	DSA	4D-CE-MRA[a]	Intermodality Agreement
Main feeders						
IMA	3	3		4	3	
Oph A	2	3		3	2	
Facial A	2	1		2	1	
Occipital A	1	1		0	1	
PCA	0	1	6/15 (40%)	1	1	8/15 (53%)
ACA	0	2		2	1	
Cerebellar A	0	0		1	0	
ICA	0	1		1	0	
Other feeders	7	3		1	6	
Tumor stain[b]						
Grade 0	0	0		0	0	
Grade 1	8	7	14/15 (93%)	6	8	13/15 (87%)
Grade 2	7	8		9	7	

Note:—IMA indicates internal maxillary artery; Oph A, ophthalmic artery; Facial A, facial artery; Occipital A, occipital artery; PCA, posterior cerebral artery; ACA, anterior cerebral artery; Cerebellar A, cerebellar artery; ICA, internal carotid artery.
[a] Consensus reading of the 2 observers.
[b] The degree of tumor stain was classified as grade 0, not visible; grade 1, visible only after the late arterial phase; and grade 2, visible from the early arterial phase.

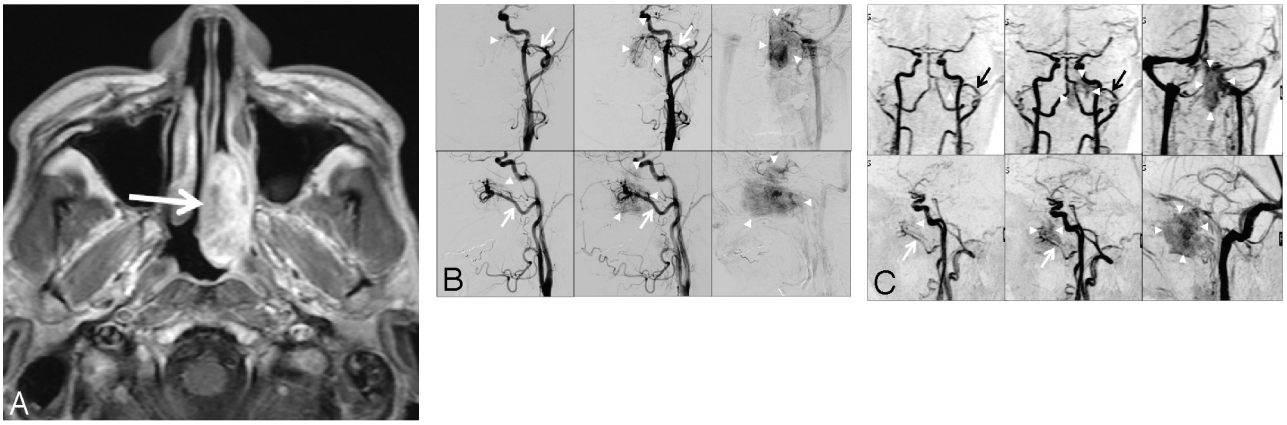

Fig 1. A 44-year-old man with juvenile angiofibroma. *A*, Axial contrast-enhanced T1-weighted MR image shows an enhanced mass in the left nasopharyngeal space (*arrow*). *B*, Anteroposterior (upper) and lateral (lower) DSA projections from the left common carotid artery during the early arterial (left), late arterial (middle), and venous (right) phase. DSA shows a tumor stain (*arrowheads*) at the early-arterial-to-venous phase; supply is from branches of the left internal maxillary artery (*arrow*). *C*, Anteroposterior (upper) and lateral (lower) projections of maximum-intensity 4D-CE-MRA images (2.9/1.4, 20° flip angle). Tumor stain (*arrowheads*) is seen from the early arterial phase (left); it is apparent in the late arterial (middle) and venous phases (right). The tumor is mainly supplied by branches from the left internal maxillary artery (*arrow*). Both readers judged that the internal maxillary artery was the main arterial feeder and that the tumor stain was grade 2.

ment was recorded as very good ($\kappa = 0.87$; 95% CI, 0.62–1.0) (Tables 1 and 2).

Discussion

We found that 4D-CE-MRA at 3T seems to be a reliable diagnostic tool for the evaluation of tumor stain in brain and head and neck tumors. Although the temporal resolution was better on DSA than on 4D-CE-MRA images, 4D-CE-MRA provided hemodynamic information regarding tumor stain at early and late arterial, parenchymal, and venous phases. Because the arteriovenous transit time in the carotid artery–brain–jugular vein circulation is 6–10 seconds,[15] high temporal resolution is required for the adequate depiction of tumor stain in the brain and in head and neck regions. Our 4D-CE-MRA sequence was based on a combination of SENSE, keyhole acquisition, half-scan, and CENTRA *k*-space sampling techniques.[8-14] This yielded a total acceleration factor of 88.8 compared with the standard contrast-enhanced MRA technique and facilitated the acquisition of MR images at a temporal resolution of 1.9 s/volume.

On the other hand, 4D-CE-MRA was not reliable for identifying feeding arteries. In our study, the spatial resolution of DSA was much higher than that of 4D-CE-MRA. Compared with the voxel size of 4D-CE-MRA images, the diameter of arterial tumor feeders is often small and the spatial resolution on these images would not be high enough to depict small feeders. Technical advances (eg, 32-channel coil, 7T MR imaging system) further increase the signal intensity–to-noise ratio[16,17]; these might improve the visualization of arterial feeders on 4D-CE-MRA images.

Information on tumor vascularity is necessary for a differential diagnosis and for planning interventional procedures.[1-7] It is also important for surgeons to know vasculature ahead of time, even without preoperative embolization to improve operative planning. On the basis of our results, 4D-CE-MRA may be equivalent to DSA at the primary diagnosis aimed at identifying the presence or absence of hypervascular tumors. However, it is not able to replace DSA in the planning of interventional procedures because of poor identification of feeding arteries.

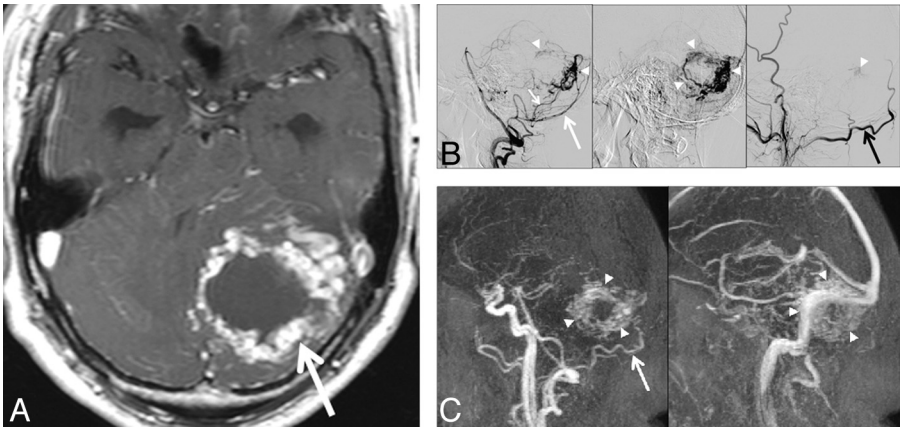

Fig 2. A 54-year-old man with cerebellar hemangioblastoma. *A,* Contrast-enhanced MR image shows a ring-enhanced mass in the left cerebellar hemisphere (*arrow*). *B,* Lateral DSA projections from the left vertebral (left, middle) and the external carotid (right) artery at the early arterial (left, right) and venous (middle) phases. DSA shows a tumor mainly supplied by branches from the posterior meningeal artery (*white arrow*). The other feeders were the posterior inferior cerebellar (*small white arrow*) and occipital (*black arrow*) arteries. Tumor stain is seen at the early arterial and venous phases (*arrowheads*). *C,* Lateral projections of maximum-intensity 4D-CE-MRA images (2.9/1.4, 20° flip angle). Tumor stain (*arrowheads*) is seen from the early arterial (left) to the venous phase (right). Both readers judged that the occipital artery (*arrow*) was the main arterial feeder and that the tumor stain was grade 2.

Table 2: Interobserver and intermodality agreement for tumor vasculature evaluation[a]

	Main Feeders	Tumor Stain
Interobserver agreement	0.283 (0.095–0.662)	0.867 (0.618–1.000)
Intermodality agreement	0.454 (0.165–0.743)	0.737 (0.409–1.000)

[a] Data are κ statistics, with 95% CIs in parentheses.

There are some limitations in our study. First, this study is a preliminary look into a 4D-CE-MRA technique in a specific subset of patients. The temporal and spatial resolution of DSA could be further improved by using smaller FOVs and frame rates of up to 30/s. DSA can also be more selectively performed. Further studies compared with DSA are required to clarify the value of this MR imaging technique. Second, we did not compare 4D-CE-MRA with conventional nonenhanced time-of-flight MRA data. Conventional MRA might yield additional information, especially with respect to the feeding artery. Third, conventional MR imaging and basic CE-MRA techniques allow identification of hypervascular lesions. Further studies would be needed to clarify the additional value of 4D-CE-MRA to these techniques. Fourth, our study did not address the actual number of vessels that supplied individual tumors. Fifth, we did not evaluate the draining veins of tumors. This information may be important for planning surgery.

Conclusions

Although 4D-CE-MRA may be a reliable tool for evaluating tumor stain in hypervascular brain and head and neck tumors, it is not able to replace DSA in planning interventional procedures.

References

1. Gemmete JJ, Ansari SA, McHugh J, et al. **Embolization of vascular tumors of the head and neck.** *Neuroimaging Clin N Am* 2009;19:181–98
2. Vogl TJ, Juergens M, Balzer JO, et al. **Glomus tumors of the skull base: combined use of MR angiography and spin-echo imaging.** *Radiology* 1994;192:103–10
3. van den Berg R, van Gils AP, Wasser MN. **Imaging of head and neck paragangliomas with three-dimensional time-of-flight MR angiography.** *AJR Am J Roentgenol* 1999;172:1667–73
4. van den Berg R, Verbist BM, Mertens BJ, et al. **Head and neck paragangliomas: improved tumor detection using contrast-enhanced 3D time-of-flight MR angiography as compared with fat-suppressed MR imaging techniques.** *AJNR Am J Neuroradiol* 2004;25:863–70
5. Arnold SM, Strecker R, Scheffler K, et al. **Dynamic contrast enhancement of paragangliomas of the head and neck: evaluation with time-resolved 2D MR projection angiography.** *Eur Radiol* 2003;13:1608–11
6. Michaely HJ, Herrmann KA, Dietrich O, et al. **Quantitative and qualitative characterization of vascularization and hemodynamics in head and neck tumors with a 3D magnetic resonance time-resolved echo-shared angiographic technique (TREAT): initial results.** *Eur Radiol* 2007;17:1101–10
7. Neves F, Huwart L, Jourdan G, et al. **Head and neck paragangliomas: value of contrast-enhanced 3D MR angiography.** *AJNR Am J Neuroradiol* 2008;29:883–39
8. Willinek WA, Hadizadeh DR, von Falkenhausen M, et al. **4D time-resolved MR angiography with keyhole (4D-TRAK): more than 60 times accelerated MRA using a combination of CENTRA, keyhole, and SENSE at 3.0T.** *J Magn Reson Imaging* 2008;27:1455–60
9. Parmar H, Ivancevic MK, Dudek N, et al. **Dynamic MRA with four-dimensional time-resolved angiography using keyhole at 3 Tesla in head and neck vascular lesions.** *J Neuroophthalmol* 2009;29:119–27
10. Nishimura S, Hirai T, Sasao A, et al. **Evaluation of dural arteriovenous fistulas with 4D contrast-enhanced MR angiography at 3T.** *AJNR Am J Neuroradiol* 2010;31:80–85
11. van Vaals JJ, Brummer ME, Dixon WT, et al. **"Keyhole" method for accelerating imaging of contrast agent uptake.** *J Magn Reson Imaging* 1993;3:671–75
12. Farb RI, McGregor C, Kim JK, et al. **Intracranial arteriovenous malformations: real-time auto-triggered elliptic centric-ordered 3D gadolinium-enhanced MR angiography—initial assessment.** *Radiology* 2001;220:244–51
13. Willinek WA, Gieseke J, Conrad R, et al. **Randomly segmented central k-space ordering in high-spatial-resolution contrast-enhanced MR angiography of the supraaortic arteries: initial experience.** *Radiology* 2002;225:583–88
14. Taschner CA, Gieseke J, Le Thuc V, et al. **Intracranial arteriovenous malformation: time-resolved contrast-enhanced MR angiography with combination of parallel imaging, keyhole acquisition, and k-space sampling techniques at 1.5 T.** *Radiology* 2008;246:871–79
15. Kim JK, Farb RI, Wright GA. **Test bolus examination in the carotid artery at dynamic gadolinium-enhanced MR angiography.** *Radiology* 1998;206:283–89
16. Parikh PT, Sandhu GS, Blackham KA, et al. **Evaluation of image quality of a 32-channel versus a 12-channel head coil at 1.5T for MR imaging of the brain.** *AJNR Am J Neuroradiol* 2011;32:365–73
17. Prudent V, Kumar A, Liu S, et al. **Human hippocampal subfields in young adults at 7.0 T: feasibility of imaging.** *Radiology* 2010;254:900–06